Laboratory Investigation (2014) 94, 1103–1113

Hepatic cytochrome *P*450 deficiency in mouse models for intrahepatic cholestasis predispose to bile salt-induced cholestasis

Cindy Kunne, Marijke de Graaff, Suzanne Duijst, Dirk R de Waart, Ronald PJ Oude Elferink and Coen C Paulusma

Progressive familial intrahepatic cholestasis (PFIC) types 1 and 3 are severe cholestatic liver diseases caused by deficiency of ATB8B1 and ABCB4, respectively. Mouse models for PFIC display mild phenotypes compared with human patients, and this can be explained by the difference in bile salt pool composition. Mice, unlike humans, have the ability to detoxify hydrophobic bile salts by cytochrome *P*450-mediated (re)hydroxylation and thus have a less toxic bile salt pool. We have crossed mouse models for PFIC1 and PFIC3 with *Hrn mice* that have a reduced capacity to (re)hydroxylate bile salts. Double transgenes were obtained by backcrossing *Atp8b1*$^{G308V/G308V}$ and *Abcb4*$^{-/-}$ mice with *Hrn* mice that have a liver-specific disruption of the *cytochrome P450 reductase* gene and therefore have markedly reduced *P*450 activity. In these mice, a more hydrophobic bile salt pool was instilled by cholic acid supplementation of the diet, and bile formation and liver pathology was studied. As opposed to single transgenes, *Atp8b1*$^{G308V/G308V}$*/Hrn* and *Abcb4*$^{-/-}$*/Hrn* mice rapidly developed strong cholestasis that was evidenced by increased plasma bilirubin and bile salt levels. The bile salt pool was more toxic in both models; *Atp8b1*$^{G308V/G308V}$*/Hrn* mice had a more hydrophobic plasma pool compared with the single transgene, whereas *Abcb4*$^{-/-}$*/Hrn* mice had a more hydrophobic biliary pool compared with the single transgene. In line with these findings, liver damage was not aggravated in *Atp8b1*$^{G308V/G308V}$*/Hrn* but was more severe in *Abcb4*$^{-/-}$*/Hrn* mice. These data indicate that bile salt pool composition is a critical determinant in the initiation and progression of cholestasis and liver pathology in PFIC1 and PFIC3. Most importantly, our data suggest that the hydrophobicity of the plasma bile salt pool is an important determinant of the severity of cholestasis, whereas the hydrophobicity of the biliary bile salt pool is an important determinant of the severity of liver pathology.

Laboratory Investigation (2014) **94,** 1103–1113; doi:10.1038/labinvest.2014.102; published online 28 July 2014

Progressive familial intrahepatic cholestasis (PFIC) types 1 and 3 are defined on basis of mutations in genes encoding two phospholipid transporting proteins that are essential in the formation of primary bile, that is, *ATP8B1* (PFIC1) and *ABCB4* (PFIC3).[1] PFIC1 patients present in the first years of life with jaundice and pruritis and suffer from progressive liver disease culminating in cirrhosis.[2] Young patients usually show a failure to thrive. Liver histology reveals bridging fibrosis but no bile duct proliferation. PFIC1 patients can develop extrahepatic symptoms, including hearing loss and diarrhea even after liver transplantation.[3] ATP8B1 is a flippase that translocates phospatidylserine from the exoplasmic to the cytosolic leaflet of biological membranes.[4,5] We and others have previously shown that ATP8B1 deficiency leads to loss of the normal phospholipid asymmetry of the canalicular membrane. As a result, the canalicular membrane becomes more sensitive to extraction of cholesterol by hydrophobic bile salts that impairs the activity of the bile salt export pump (ABCB11) and, as a consequence, causes cholestasis.[6] PFIC3 patients suffer from a chronic and progressive cholestasis with high serum γ-glutamyltransferase levels; liver histology reveals fibrosis that progresses into cirrhosis with portal inflammation and strong bile duct proliferation. In addition, milder mutations in *ABCB4* have been shown to predispose to intrahepatic cholestasis of pregnancy, cholelithiasis, adult biliary cirrhosis, primary sclerosing cholangitis, and drug- and cytokine-induced cholestatic injury.[7] ABCB4 is a floppase that translocates phospatidylcholine from the cytosolic to the exoplasmic leaflet of the canalicular membrane.[8,9] Phospatidylcholine in the exoplasmic leaflet of the apical membrane can be extracted by bile salt micelles to form mixed micelles, thus reducing the detergent effect of bile

Tytgat Institute for Liver and Intestinal Research, Academic Medical Center, Amsterdam, The Netherlands
Correspondence: Dr C Kunne, PhD, Tytgat Institute for Liver and Intestinal Research, Academic Medical Center, S2-166, Meibergdreef 69-71, 1105BK Amsterdam, The Netherlands.
E-mail: c.kunne@amc.uva.nl

Received 21 January 2014; revised 19 June 2014; accepted 29 June 2014

salts.[9] Consequently, ABCB4 deficiency results in bile that is cytotoxic to the cells lining the biliary tree. For both PFIC1 and PFIC3, mouse models have been generated, that is, *Atp8b1*$^{G308V/G308V}$ and *Abcb4*$^{-/-}$ mice.[10–12] In contrast to PFIC1 patients, *Atp8b1*$^{G308V/G308V}$ mice develop very little liver pathology and are only mildly cholestatic.[10,13] Similar to patients, in *Atp8b1*$^{G308V/G308V}$ mice the canalicular content has a coarsely granular appearance upon EM that is reminiscent of Byler's bile;[6] in addition, these mice also suffer from hearing loss caused by a progressive degeneration of stereocilia and cochlear hair cells.[14] *Abcb4*$^{-/-}$ mice display mild fibrosis that does not progress into cirrhosis; mice do display cholangiopathy, that is, periductal inflammation and bile duct proliferation. Still, liver failure does not occur during the lifespan of these animals.[11,15]

Overall, these mouse models display much less severe phenotypes compared with those of human patients.[11,12] A likely explanation for this discrepancy may be the difference in bile salt pool composition. The cytotoxic effect of bile depends on the hydrophobicity[16,17] of the bile salt pool that is different in mice and humans. In contrast to humans, mice are capable of rehydroxylating toxic, dihydroxy bile salts. Therefore, the bile salt pool of mice mainly consists of trihydroxy bile salts, whereas the human bile salt pool contains more dihydroxy bile salts, including secondary bile salts that are formed in the gut by bacterial dehydroxylation of bile salts.

Bile salt synthesis and hydroxylation are mediated by the cytochrome *P*450 monoxygenase system in hepatocytes.[18] All cytochrome *P*450s receive an electron from a single donor, a reaction mediated by the cytochrome *P*450 oxidoreductase (Cpr).[19,20] Whole body deletion of *cytochrome P450 oxidoreductase* inactivates all cytochrome *P*450s and is embryonic lethal.[21] Henderson *et al*[20] have generated a hepatocyte-specific *cytochrome P450 oxidoreductase* knockout mouse, also termed hepatic reductase null (*Hrn)* mouse. In this model, bile salt synthesis and (re)hydroxylation are reduced by 95%. Endogenous bile salt output in *Hrn* mice was threefold reduced compared with wild-type (WT) mice, likely because of strongly reduced bile salt synthesis. In contrast to WT mice in which the bile salt pool consists of 90% trihydroxy and 10% dihydroxy bile salts, the bile salt pool of *Hrn* mice contains ~55% trihydroxy and 45% dihydroxy bile salts after feeding these mice a cholic acid-supplemented diet.[22]

We hypothesized that backcrossing *Hrn* mice with the existing mouse models for PFIC1 and PFIC3 would render mouse models that predispose to cholestatic liver disease upon instillment of a more hydrophobic bile salt pool.

MATERIALS AND METHODS

Animals

Ethics statement

All animal experiments were approved by the institutional animal care and use committee of the Academic Medical Center.

C57bl/6 *Cpr*$^{lox/lox}$ + *Cre*^{ALB} (*Hrn*) animals were bred with C57bl/6 *Atp8b1*$^{G308V/G308V}$ mutant mice or FVB *Abcb4*$^{-/-}$ to obtain C57bl/6 *Atp8b1*$^{G308V/G308V}$ *Cpr*$^{lox/lox}$ + *Cre*^{ALB} (further designated as *Atp8b1*$^{G308V/G308V}$/*Hrn*) and C57bl/6/FVB *Abcb4*$^{-/-}$/*Cpr*$^{lox/lox}$ + *Cre*^{ALB} (further designated as *Abcb4*$^{-/-}$/*Hrn*), respectively. Littermates and WT mice (Harlan) were included as controls. The animals were kept in a pathogen-free environment on a controlled 12 h light/dark regime in the animal facility of the Academic Medical Center Amsterdam. Male mice were fed a standard purified semi-synthetic diet (K4068.02; Arie Blok diervoeders, Woerden, The Netherlands) either or not supplemented with 0.03% cholic acid (CA) and water *ad libitum* starting from weaning ($t = 0$). *Abcb4*$^{-/-}$/*Hrn* were fed for 8 weeks, whereas *Atp8b1*$^{G308V/G308V}$/*Hrn* mice were fed a control diet for 4 weeks followed by a 0.03% CA-supplemented diet for an additional 4 weeks. Blood was taken every 2 weeks. After the feeding period, bile was collected after which the animals were killed and blood and livers were collected.

Bile Collection

In order to obtain bile, mice were anesthetized and placed on a thermostatted heating pad to remain body temperature. The common bile duct was closed with a ligature and the gallbladder cannulated. Bile was collected in fractions of 10 or 15 min. At the end of the experiment blood and liver were harvested.

Plasma Biochemistry

Plasma biochemistry was performed by the routine laboratory of clinical chemistry of the AMC.

Bile Salt, Phospholipid, and Cholesterol Assays

Biliary bile salts, choline-containing phospholipids, and cholesterol were determined enzymatically using a Novostar analyzer (BMG Labtech GmbH, Offenburg, Germany) as described earlier.[6] Hepatic bile salts were extracted after homogenizing in water using acetonitrile and dissolved in 25% methanol. Bile salt species were determined by reverse phase HPLC using a nano quantity analyte detector (NQAD) QT-500 (Quant Technologies, Blaine, MN, USA). In brief, bile was injected after dilution with water. Then, 100 μl was applied to a Hypersil C18, 3 μm, 15 cm HPLC column (Thermo Scientific, Breda, The Netherlands). The starting eluent consisted of 6.8 mM ammonium formate (pH 3.9), followed by several steps of linear gradients to different concentrations of acetonitrile (ACN; Biosolve, Valkenswaard, The Netherlands): 1 min 27% ACN, 13 min 42% ACN, 19 min 42% ACN, 20 min 60% ACN, 26 min 66% ACN, 27 min 80% ACN, 29 min 80% ACN, and 30 min 0% ACN. Detection was performed using a NQAD QT-500. Quantification of the different bile salt species was performed by using a calibration curve for all different bile salt species.

Quantitative PCR Analysis of Gene Expression

Liver tissue was snap frozen and stored at $-80\,^{\circ}C$. RNA was isolated using Trizol reagent (Invitrogen, Bleiswijk, The Netherlands). The cDNA synthesis was transcribed using locked oligo-dT primers and Superscript III reverse transcriptase (Invitrogen). Quantitative PCR was performed using a Lightcycler 2.0 with the Fast Start DNA Master^{Plus} SYBR Green I kit (Roche, Woerden, The Netherlands). Expression levels were normalized for cyclophylin/hypoxanthine-guanine phosphoribosyltransferase.

Immunohistochemistry

Livers were fixed in 4% paraformaldehyde solution and embedded in paraffin wax. Then, 7 μm sections were stained with sirius red (collagen deposition), CK19 (bile duct proliferation), or Ki67 (cell proliferation). Oil red O (lipids) stainings were performed on frozen sections.

Liver Triglycerides

Liver triglycerides were extracted by a chloroform/methanol extraction method adapted from Srivastava *et al.*[23] and measured using a Trig/GB-kit (Roche).

Liver Hydroxyprolines

Liver hydroxyprolines were extracted and measured according to van Westrhenen *et al.*.[24] After extraction, the amino acids (hydroxyprolines) were measured using HPLC and fluorescent detection.

Statistical Analysis

All data are given as means ± s.e.m. or indicated else. Significance was tested using two-way ANOVA with Bonferroni's correction for multiple testing, considering statistical significance when $P<0.05$.

RESULTS

We generated double transgenic mouse models for PFIC1 and PFIC3 by crossing *Atp8b1*$^{G308V/G308V}$ and *Abcb4*$^{-/-}$, respectively, with hepatic reductase-null (*Hrn*) mice. On top of deficiency for the respective transport proteins (ATP8B1 or ABCB4), both mouse models are for ~95% impaired in the synthesis of primary bile salts and the rehydroxylation of secondary bile salts (*Hrn*). The characteristics of the single transgenic *Hrn* mice with regard to bile formation have been described before.[22] In the double transgenic mice, we instilled a more hydrophobic bile salt pool by feeding 0.03% CA-supplemented diets directly from weaning.

At Weaning, *Atp8b1*$^{G308V/G308V}$/*Hrn* Mice Are Extremely Sensitive to Bile Salt Feeding

When *Atp8b1*$^{G308V/G308V}$/*Hrn* mice were fed a 0.03% CA-supplemented diet directly from weaning, they died within a week after the start of the diet. Because the mice died during the night, the cause of premature death could not be established. Thus, we hypothesized that premature death in these neonates could be the consequence of the combination of ATP8B1 deficiency, a more toxic bile salt pool upon CA feeding and low *Abcb4* expression. Indeed, compared with 8-week-old mice, the naive 3-week-old WT mice have an ~10-fold lower *Abcb4* expression (Supplementary Figure 1). In combination with the CA feeding, this possibly accounted for the premature death of these double transgenes. We therefore shifted to a protocol in which the animals were first fed a control diet from weaning for 4 weeks followed by a 0.03% CA-supplemented diet for another 4 weeks. Using this protocol the mice survived and all further experiments with these mice were done in this manner.

CA-Fed *Atp8b1*$^{G308V/G308V}$/*Hrn* Mice Are Cholestatic and Display Mild Liver Damage

Mice fed control diets displayed normal weight gain, plasma biochemistry, and bile flow (data of control-fed animals are not shown unless indicated). In contrast to WT, *Hrn*, and *Atp8b1*$^{G308V/G308V}$ mice, *Atp8b1*$^{G308V/G308V}$/*Hrn* mice failed to gain and even lost weight after the start of the experimental diet at week 4 (Figure 1a). After 4 weeks of CA feeding, *Atp8b1*$^{G308V/G308V}$/*Hrn* mice displayed strongly enhanced plasma bilirubin levels compared with *Atp8b1*$^{G308V/G308V}$, WT, and *Hrn* controls (Figure 1b). Plasma alanine transaminases (ALT; Figure 1c) and alkaline phosphatase (AP; Figure 1d) were mildly elevated. Compared with 8-week-old mice, plasma AP levels were elevated in 3-week-old mice, a consequence of enhanced osteoblast activity because of bone growth. Plasma bile salt levels were strongly elevated compared with *Atp8b1*$^{G308V/G308V}$ mice (Figure 1e). Bile flow of *Atp8b1*$^{G308V/G308V}$/*Hrn* was strongly (approximately threefold) reduced compared with controls but comparable to *Atp8b1*$^{G308V/G308V}$ single mutant mice (Figure 2a). Biliary bile salt output, on the other hand, over the entire period of bile collection, was not different between the different genotypes (Figure 2b). The bile salt-independent flow for *Atp8b1*$^{G308V/G308V}$/*Hrn*, *Atp8b1*$^{G308V/G308V}$, *Hrn*, and WT was extracted from the y-intercept of Supplementary Figure 2A and was 0.35 ± 0.06, 0.21 ± 0.08, 1.12 ± 0.06, and 1.11 ± 0.07 μl/min × g liver, respectively. Because of >15% body weight loss in the *Atp8b1*$^{G308V/G308V}$/*Hrn*, the experiment had to be terminated 4 weeks after the start of the experimental diet. Liver weights of both *Atp8b1*$^{G308V/G308V}$/*Hrn* and *Atp8b1*$^{G308V/G308V}$ mice were increased compared with WT and *Hrn*. Liver to body weight ratios were more than twofold higher compared with WT (Table 1). These data indicate that, compared with *Atp8b1*$^{G308V/G308V}$ mice, *Atp8b1*$^{G308V/G308V}$/*Hrn* mice developed a much more severe cholestatic phenotype without a strong aggravation of hepatic damage.

CA-Fed *Abcb4*$^{-/-}$/*Hrn* Are Cholestatic and Develop Severe Liver Damage

Abcb4$^{-/-}$/*Hrn* mice showed normal growth on both control (data of control-fed animals are not shown unless indicated) and CA-supplemented diets when compared with *Abcb4*$^{-/-}$,

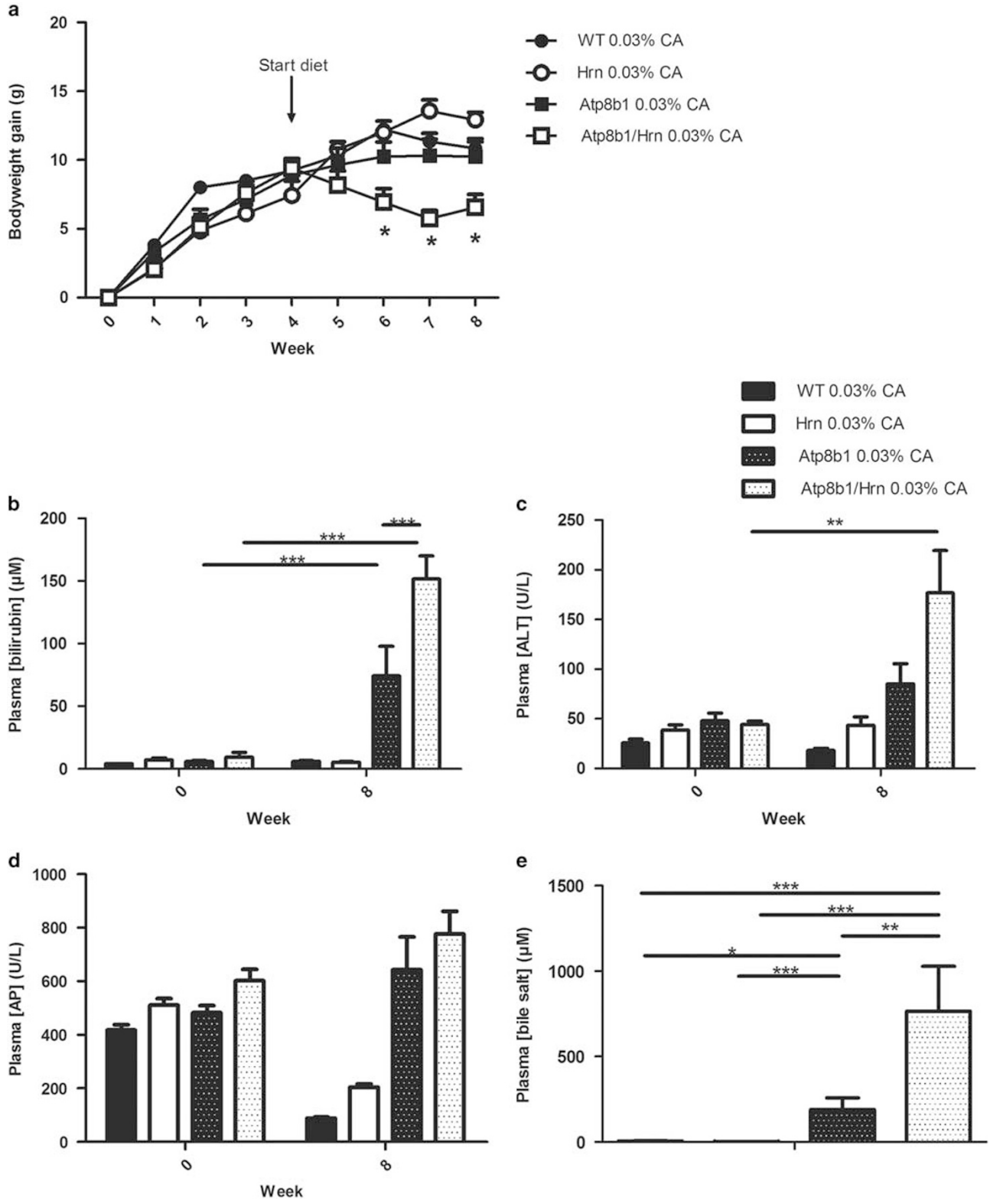

Figure 1 Characteristics of *Atp8b1*$^{G308V/G308V}$*/Hrn* mice. Mice were fed semisynthetic control diet for 4 weeks, starting from weaning, followed by 0.03% CA-supplemented diet for 4 weeks. (**a**) Body weight gain in time ($n = 3$–8), (**b**) plasma bilirubin ($n = 4$–11), (**c**) plasma ALT ($n = 5$–13), and (**d**) plasma alkaline phosphatase (AP) at the start (week 0) and at the end (week 8) of the feeding period. (**e**) Total plasma bile salt concentration ($n = 3$–7) is plotted. Data are shown as mean ± s.e.m. *$P < 0.05$; **$P < 0.001$; ***$P < 0.0001$.

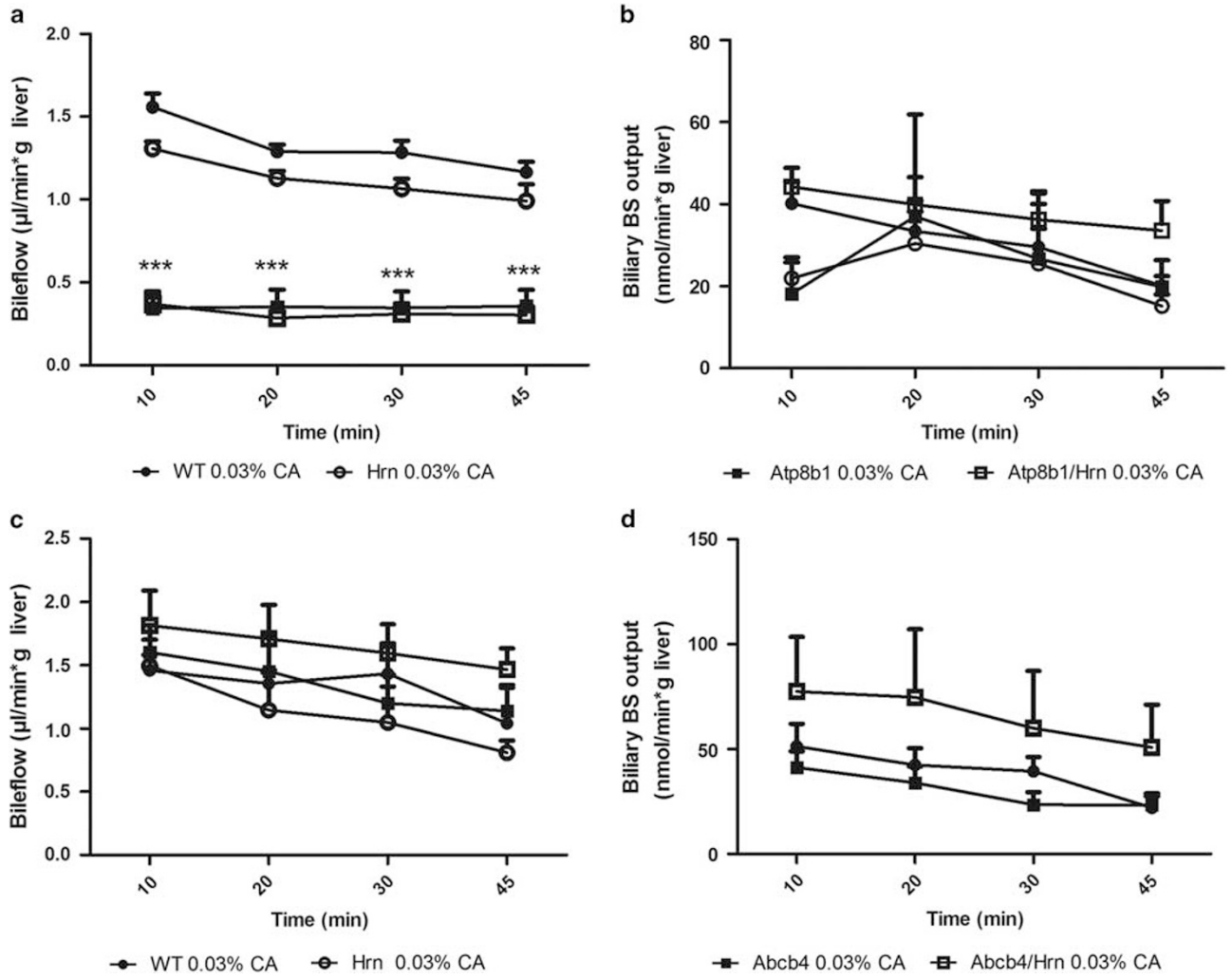

Figure 2 Bile flow and biliary bile salt output. At the end of the bile salt feeding period, gallbladders were cannulated and bile was sampled for 45 min. From the samples, bile flow was calculated and bile salts were measured. (**a**) Bile flow and (**b**) biliary bile salt output in wild-type ($n=9$), *Hrn* ($n=6$), *Atp8b1*$^{G308V/G308V}$ ($n=3$), and *Atp8b1*$^{G308V/G308V}$*/Hrn* mice ($n=7$). (**c**) Bile flow and (**d**) biliary bile salt output in wild-type ($n=4$), *Hrn* ($n=4$ for flow), *Abcb4*$^{-/-}$ ($n=7$), and *Abcb4*$^{-/-}$*/Hrn* ($n=4$) mice. Data are shown as mean ± s.e.m.

Table 1 Liver weight and liver to body weight ratios in 0.03% cholic acid-fed mice

	WT ($n=17$)	*Hrn* ($n=10$)	*Atp8b1*$^{G308V/G308V}$ ($n=4$)	*Atp8b1*$^{G308V/G308V}$*/Hrn* ($n=6$)	*Abcb4*$^{-/-}$ ($n=8$)	*Abcb4*$^{-/-}$*/Hrn* ($n=6$)
Liver weight	1.39 ± 0.05	1.68 ± 0.06[a]	2.21 ± 0.12[b,c]	1.93 ± 0.10[b,d]	2.08 ± 0.43[b,c]	2.91 ± 0.35[b,e,f]
Liver/body weight ratio	5.74 ± 0.11	7.27 ± 0.15[a]	12.157 ± 0.70[b,c]	12.89 ± 0.52[b,c]	7.48 ± 0.39[b]	10.82 ± 0.61[b,c,g]

At the end of the bile salt feeding period, mice were killed and liver weight and body weight were determined. Data are given as mean ± s.e.m. Significance was tested using Student's *t*-test.
[a]$P<0.001$ compared with WT.
[b]$P<0.0001$ compared with WT.
[c]$P<0.0001$ compared with Hrn.
[d]$P<0.05$ compared with Hrn.
[e]$P<0.001$ compared with Hrn.
[f]$P<0.05$ compared with *Abcb4* $^{-/-}$.
[g]$P<0.001$ compared with *Abcb4* $^{-/-}$.

WT, and *Hrn* control mice (Figure 3a). In contrast to *Abcb4*$^{-/-}$ mice, plasma bilirubin levels of *Abcb4*$^{-/-}$*/Hrn* mice were mildly increased already at weaning and were further increased after 8 weeks of CA-supplemented diet (Figure 3b). Plasma ALT (Figure 3c), AP (Figure 3d), and plasma bile salt levels (Figure 3e) were strongly elevated in

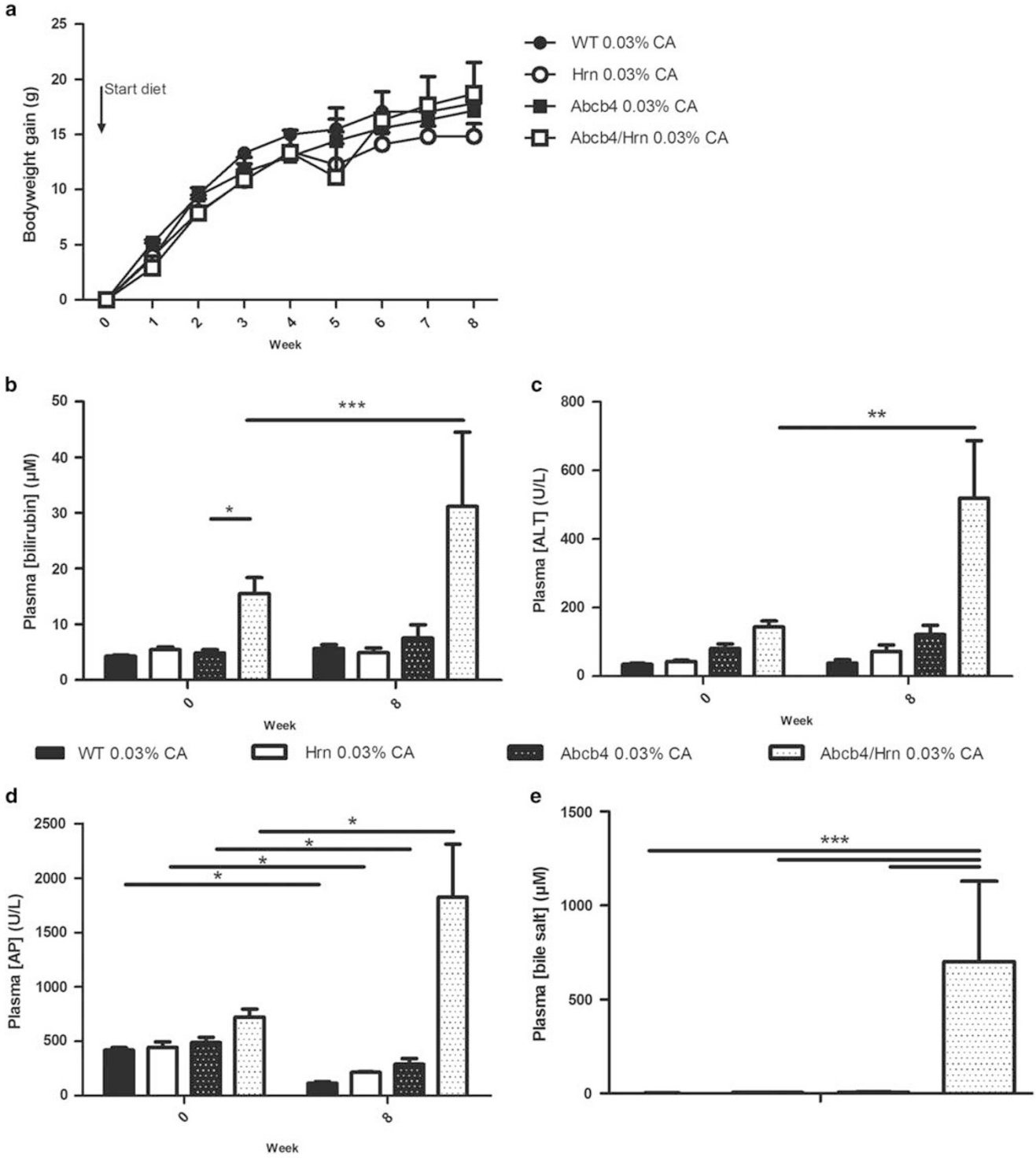

Figure 3 Characteristics of *Abcb4*$^{-/-}$*/Hrn* mice. Mice were fed control diet or 0.03% CA-supplemented diet for 8 weeks starting from weaning. (**a**) Body weight gain ($n = 3$–8), (**b**) plasma bilirubin ($n = 4$–16), (**c**) plasma ALT ($n = 4$–17), and (**d**) plasma AP at the start (week 0) and at the end (week 8) of the feeding period. (**e**) Total plasma bile salt concentration ($n = 3$–8) is plotted. Data are shown as mean ± s.e.m. *$P < 0.05$; **$P < 0.001$; ***$P < 0.0001$.

Abcb4$^{-/-}$*/Hrn*, but not in *Abcb4*$^{-/-}$ mice. Liver to body weight ratios of both *Abcb4*$^{-/-}$*/Hrn* and *Abcb4*$^{-/-}$ mice were increased compared with WT (Table 1). In contrast to mice with ATP8B1 deficiency, no significant differences in bile flow and biliary bile salt output were observed in *Abcb4*$^{-/-}$ and *Abcb4*$^{-/-}$*/Hrn* compared with WT (Figures 2c and d, respectively). Because of the variation in bile flow and bile salt output data, it was not possible to derive a significant bile salt-independent flow (Supplementary Figure 2B). Collectively, these data indicate that cholestasis and hepatic damage are aggravated in *Abcb4*$^{-/-}$*/Hrn* double transgenes compared with *Abcb4*$^{-/-}$ single transgenes.

Plasma and Biliary Bile Salt Species in CA-Fed *Atp8b1*$^{G308V/G308V}$*/Hrn* and *Abcb4*$^{-/-}$*/Hrn* Mice

We determined plasma and biliary bile salt species at the end of the bile salt feeding period. Plasma bile salts in *Atp8b1*$^{G308V/G308V}$*/Hrn* mice predominantly consisted of TC (~90% of total) and TβMC (~7% of total; Table 2 and Supplementary Figure 3A). Low concentrations of the secondary bile salt TDC (~0.4% of total) were detected. In *Atp8b1*$^{G308V/G308V}$ mice, plasma TC and TβMC made up ~70% and 20% of total bile salts, respectively. Biliary bile salts in *Atp8b1*$^{G308V/G308V}$*/Hrn* mice predominantly consisted of TC (~90% of total) and TβMC (~9% of total), whereas in *Atp8b1*$^{G308V/G308V}$ mice TC and TβMC made up ~55% and ~40% of total biliary bile salts, respectively (Table 3 and Supplementary Figure 3B). Compared with the single transgenes, the bile salt hydrophobicity index (HI) of plasma was significantly elevated, whereas the HI of bile was unaltered in the double transgenes, indicating that the plasma bile salt pool was more hydrophobic (Tables 1 and 2).

The plasma bile salt pool of *Abcb4*$^{-/-}$*/Hrn* mice consisted predominantly of TC (~90% of total) and TβMC (~7% of total; Table 2 and Supplementary Figure 3C). Plasma bile salt species in *Abcb4*$^{-/-}$ single knockout mice were similar to those of WT and *Hrn* control animals, with predominantly TC (~60%) and TβMC (~23%). Biliary bile salts in *Abcb4*$^{-/-}$*/Hrn* mice predominantly consisted of TC (~90%) and low concentrations of TDC (~2.5%; Table 3 and Supplementary Figure 3D), whereas in *Abcb4*$^{-/-}$ mice TC and TβMC made up ~75% and ~20% of total biliary bile salts, respectively. Compared with the single transgene, the biliary HI, but not the plasma HI, was elevated in the double transgenes indicative of a more hydrophobic biliary bile salt pool (Tables 1 and 2). Plasma bile salt profiles of control-fed mice are depicted in Supplementary Figures 3E and F.

Liver Histology in CA-Fed *Atp8b1*$^{G308V/G308V}$*/Hrn* and *Abcb4*$^{-/-}$*/Hrn* Mice

Sirius red staining (collagen deposition) of liver showed no fibrosis in *Atp8b1*$^{G308V/G308V}$*/Hrn* or *Atp8b1*$^{G308V/G308V}$

Table 2 Plasma bile salt species in 0.03% cholic acid-fed mice

	WT ($n=3$)	*Hrn* ($n=10$)	*Atp8b1*$^{G308V/G308V}$ ($n=4$)	*Atp8b1*$^{G308V/G308V}$*/Hrn* ($n=6$)	*Abcb4*$^{-/-}$ ($n=8$)	*Abcb4*$^{-/-}$*/Hrn* ($n=5$)
Plasma total bile salts (μM)	4.1 ± 2.2	3.9 ± 1.0	187.8 ± 70.1	764.7 ± 264.0	6.3 ± 1.5	840.4 ± 496.0
Species (% of total)						
Tauro-α-muricholate	14.4 ± 8.3	6.3 ± 1.6	10.9 ± 7.8	1.2 ± 0.9	0.7 ± 0.2	2.1 ± 0.6
Tauro-β-muricholate	11.9 ± 6.9	21.5 ± 5.0	22.8 ± 1.5	12.3 ± 4.8	20.2 ± 2.7	8.7 ± 4.2
Tauroursodeoxycholate	0.4 ± 0.2	0.3 ± 0.2	1.1 ± 1.0	0.4 ± 0.2	1.7 ± 0.9	4.0 ± 3.9
Taurocholate	71.3 ± 2.3	52.7 ± 7.3	47.8 ± 16.1	81.9 ± 7.4	46.9 ± 7.0	76.4 ± 8.8
Taurochenodeoxycholate	n.d.	3.1 ± 2.1	0.6 ± 0.5	1.2 ± 1.0	n.d.	1.9 ± 1.2
Ω-Muricholate	n.d.	0.9 ± 0.7	0.9 ± 0.6	n.d.	0.4 ± 0.4	1.6 ± 1.2
Taurodeoxycholate	n.d.	13.0 ± 6.1	1.2 ± 1.2	0.3 ± 0.2	13.6 ± 6.9	5.1 ± 4.0
α-Muricholate	n.d.	0.7 ± 0.7	1.2 ± 0.7	0.1 ± 0.02	n.d.	n.d.
β-Muricholate	n.d.	n.d.	5.5 ± 3.2	0.2 ± 0.09	n.d.	0.1 ± 0.01
Cholate	1.9 ± 1.1	1.4 ± 1.4	8.0 ± 4.2	1.6 ± 0.6	n.d.	0.1 ± 0.08
Chenodeoxycholate	n.d.	n.d.	n.d.	0.7 ± 0.9	16.5 ± 3.9	0.1 ± 0.08
Deoxycholate	n.d.	n.d.	n.d.	n.d.	n.d.	n.d.
Hydrophobicity index	− 0.21 ± 0.1	− 0.13 ± 0.06	− 0.20 ± 0.005	− 0.06 ± 0.02[a]	0.03 ± 0.09	− 0.06 ± 0.06[b]

Plasma bile salt species of cholic acid-fed mice were determined by HPLC analyses and are expressed as percentage of total bile salt. For clarity, total plasma bile salt concentrations are indicated. Hydrophobicity indices were calculated using the individual hydrophobicity indices as determined by Heuman.[28] Data are given as mean ± s.e.m.

[a] $P=0.0016$ for *Atp8b1*$^{G308V/G308V}$ *versus Atp8b1*$^{G308V/G308V}$*/Hrn*.

[b] $P=0.49$ for *Abcb4* $^{-/-}$ *versus Abcb4*$^{-/-}$*/Hrn* using Student's *t*-test.; n.d., not detectable.

Table 3 Biliary bile salt species in 0.03% cholic acid-fed mice

	WT ($n=8$)	*Hrn* ($n=9$)	*Atp8b1*$^{G308V/G308V}$ ($n=3$)	*Atp8b1*$^{G308V/G308V}$/Hrn ($n=6$)	*Abcb4*$^{-/-}$ ($n=4$)	*Abcb4*$^{-/-}$/*Hrn* ($n=5$)
Biliary total bile salts (mM)	84.2 ± 19.7	148.8 ± 24.6	114.3 ± 84.0	107.0 ± 37.7	54.7 ± 15.5	64.0 ± 19.3
Species (% of total)						
Tauro-α-muricholate	2.3 ± 0.2	4.4 ± 1.0	n.d.	1.0 ± 0.9	0.9 ± 0.5	1.1 ± 0.2
Tauro-β-muricholate	17.5 ± 1.5	4.4 ± 1.6	32.3 ± 8.6	27.4 ± 11.0	19.3 ± 2.1	3.6 ± 0.4
Tauroursodeoxycholate	4.3 ± 0.5	3.1 ± 0.7	1.9 ± 1.9	0.6 ± 0.5	3.1 ± 1.5	n.d.
Taurocholate	73.2 ± 2.3	68.2 ± 3.6	63.3 ± 11.5	65.7 ± 15.0	75.2 ± 3.8	91.1 ± 1.2
Taurochenodeoxycholate	1.6 ± 0.3	12.5 ± 1.4	2.1 ± 1.0	1.1 ± 1.0	0.2 ± 0.1	0.5 ± 0.1
Taurodeoxycholate	1.1 ± 0.2.	7.1 ± 3.7	0.3 ± 0.3	4.2 ± 5.1	1.3 ± 0.2	3.6 ± 1.0
Hydrophobicity index	− 0.11 ± 0.03	0.01 ± 0.04	− 0.25 ± 0.07	− 0.20 ± 0.07[a]	− 0.16 ± 0.03	− 0.01 ± 0.01[b]

Biliary bile salt species of cholic acid-fed mice were determined by HPLC analyses and are expressed as percentage of total bile salt. For clarity, total biliary bile salt concentrations are indicated. Hydrophobicity indices were calculated using the individual hydrophobicity indices as determined by Heuman.[28] Data are given as mean ± s.e.m.
[a]$P=0.63$ for *Atp8b1*$^{G308V/G308V}$ *versus* *Atp8b1*$^{G308V/G308V}$/*Hrn*.
[b]$P=0.0003$ for *Abcb4*$^{-/-}$ *versus* *Abcb4*$^{-/-}$/*Hrn* using Student's *t*-test; n.d., not detectable.

mice (Figure 4a), confirmed by quantification of hepatic hydroxyproline levels (Figure 4b). Bile duct proliferation, evidenced by cytokeratin 19 (CK19) staining, was slightly increased in *Atp8b1*$^{G308V/G308V}$/*Hrn* mice compared with controls (Supplementary Figure 4A). No hepatocyte proliferation was observed, as shown by Ki67 immunostaining (Supplementary Figure 4B).

Sirius red staining of livers of *Abcb4*$^{-/-}$ livers indicated portal fibrosis that was aggravated in livers of *Abcb4*$^{-/-}$/*Hrn* mice, where portal-bridging fibrosis was observed (Figure 4a). Quantification of liver hydroxyproline confirmed that the fibrosis in CA-fed *Abcb4*$^{-/-}$/*Hrn* mice was more severe than in *Abcb4*$^{-/-}$ mice, and was already present in control-fed *Abcb4*$^{-/-}$/*Hrn* mice to a similar level as in CA-fed *Abcb4*$^{-/-}$ mice (Figure 4c). Compared with livers of *Abcb4*$^{-/-}$ mice, livers of *Abcb4*$^{-/-}$/*Hrn* mice displayed extensive areas of CK19 staining, especially in the portal tracts (Supplementary Figure 4A); this coincided with a significant induction of *Ck19* mRNA levels and is indicative for bile duct proliferation (not shown). In addition, hepatocyte proliferation (by Ki67) was strongly increased in livers of *Abcb4*$^{-/-}$/*Hrn* mice, evidenced by extensive nuclear staining and elevated *Ki67* mRNA levels (Supplementary Figure 4B and data not shown).

DISCUSSION

In this study we have characterized novel mouse models for PFIC1 and PFIC3 disease, *Atp8b1*$^{G308V/G308V}$/*Hrn* and *Abcb4*$^{-/-}$/*Hrn* double transgenic mice, in which we have instilled a more hydrophobic bile salt pool by feeding 0.03% CA-supplemented diets. Our data indicate that the cholestatic phenotypes of the double transgenes were aggravated compared with those of the single transgenes. As expected, the more hydrophobic bile salt pool is responsible for these aggravated phenotypes.

For instance, *Atp8b1*$^{G308V/G308V}$/*Hrn* mice displayed failure to thrive and accumulated higher concentrations of bilirubin and bile salts compared with *Atp8b1*$^{G308V/G308V}$ single mutants. This coincides with a strong reduction in bile flow. Feeding diets supplemented with 0.03% CA was toxic to *Atp8b1*$^{G308V/G308V}$/*Hrn* mice during weaning, but not when started 4 weeks after weaning. Although we cannot exclude that the mice died from impaired intestinal fat- and fat-soluble vitamin uptake because of reduced intestinal bile salt concentrations, we favor the hypothesis of the combination of a toxic bile salt pool and very low *Abcb4* expression in an ATP8B1-deficient background. Apparently, in 3-week-old naive mice, the low *Abcb4* levels (Supplementary Figure 1) guarantee sufficient biliary phosphatidylcholine excretion to protect the canalicular membrane from luminal bile salt insult. However, when fed a CA diet, the mice will have a more hydrophobic bile salt pool that, in combination with low *Abcb4* expression and deficiency of ATP8B1, renders the canalicular membrane more sensitive to cholestasis. Liver pathology in adult *Atp8b1*$^{G308V/G308V}$/*Hrn mice* was slightly aggravated compared with single transgenes, but still very mild, that may be because of the short experimental period.

Conversely, *Abcb4*$^{-/-}$/*Hrn* double transgenic mice developed a more severe phenotype than *Abcb4*$^{-/-}$ single transgenic mice. Liver pathology was much more severe compared with pathology in *Abcb4*$^{-/-}$ mice, evidenced by portal-bridging fibrosis and extensive hepatocyte and bile

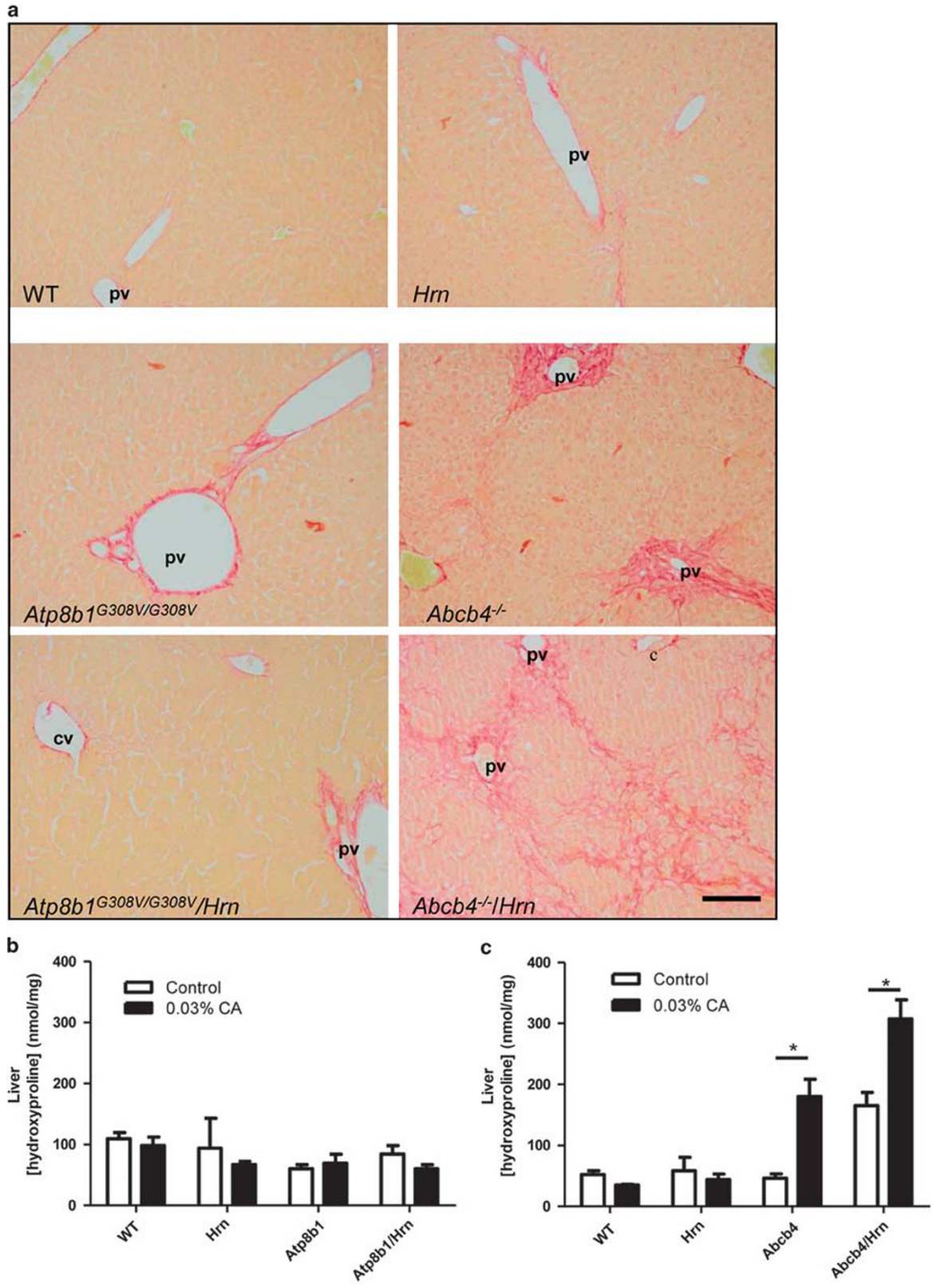

Figure 4 Liver fibrosis. Liver pathology of mice fed 0.03% CA-supplemented diets. After the feeding period, mice were killed and livers were collected. (**a**) Livers were stained for collagen with picrosirius red (PSR) (genotypes are depicted in the pictures). Hydroxyprolines were extracted and measured using HPLC. (**b**) Liver hydroxyprolines from WT, *Hrn*, *Atp8b1*$^{G308V/G308V}$, and *Atp8b1*$^{G308V/G308V}$*/Hrn* mice ($n = 3$–9). (**c**) Liver hydroxyprolines from WT, *Hrn*, *Abcb4*$^{-/-}$, and *Abcb4*$^{-/-}$*/Hrn* mice ($n = 3$–10). Bar represents 100 nm; cv, central vein; pv, portal vein.

duct proliferation. Paradoxically, *Abcb4*$^{-/-}$*/Hrn* mice have increased bile flow and bile salt output that (on top of the strongly enhanced bile salt pool) may be explained by the extensive bile duct proliferation in these animals. In relation to this, we have previously shown that bile salt-independent bile flow was increased in the single *Abcb4*$^{-/-}$ mice.[25] Indeed, we also observed an increased bile salt-independent flow in *Abcb4*$^{-/-}$*/Hrn* mice (Supplementary Figure 2B). Obviously, the more hydrophobic bile salt pool causes more hepatocyte and cholangiocyte damage that induces massive fibrosis and hepatocyte and cholangiocyte proliferation in these double transgenes.

An interesting observation is the much stronger liver pathology in CA-fed *Abcb4*$^{-/-}$*/Hrn* mice compared with CA-fed *Atp8b1*$^{G308V/G308V}$*/Hrn* mice. This was clear from higher ALT and AP levels, stronger fibrosis, and more hepatocellular proliferation. Bile salt-induced liver pathology in *Abcb4*$^{-/-}$*/Hrn* mice is in particular caused by damage to cells lining the biliary tree. Thus, membranes of cells lining the biliary tree have to defend themselves against bile salts. Research in the past decade has demonstrated that hepatocytes and bile duct epithelial cells achieve this defense by two mechanisms.[9] One important line of defense is via biliary, ABCB4-mediated excretion of considerable amounts of phosphatidylcholine that associates with bile salt micelles to reduce the detergent activity of these micelles. *Abcb4*$^{-/-}$ mice develop liver pathology because they have no phospholipids in bile. Importantly, liver pathology in *Abcb4*$^{-/-}$ mice was aggravated when the biliary bile salt pool was more hydrophobic.[26] A second line of defense is to maintain a rigid, detergent-resistant membrane structure. The canalicular membrane is enriched in cholesterol and sphingomyelin that allows tight packing of membrane lipids and makes the membrane resistant to bile salt-mediated lipid extraction. We have previously shown that ATP8B1 is essential in maintaining detergent resistance of this membrane domain;[6] the canalicular membrane in *Atp8b1*$^{G308V/G308V}$ mice was prone to elution of membrane cholesterol and phospholipids, a phenotype that depended on bile salt hydrophobicity, as infusion of the hydrophilic bile salt tauroursodeoxycholate did not result in cholesterol/phospholipid elution. Still, *Atp8b1*$^{G308V/G308V}$ mice have very little liver pathology (compared with *Abcb4*$^{-/-}$ mice) because as a consequence of the extraction of cholesterol from the canalicular membrane there is a severe impairment of BSEP and MRP2 function and therefore strong cholestasis (see Figure 1). This development of cholestasis was much more prominent in *Atp8b1*$^{G308V/G308V}$*/Hrn* mice. Although the impaired secretory function causes cholestasis, it does prevent strong damage by bile salts to canalicular and cholangiocyte membranes from the luminal side. The consequence of the strong cholestasis is also that there is more retention of bile salt in the hepatocytes of *Atp8b1*$^{G308V/G308V}$*/Hrn* mice compared with *Abcb4*$^{-/-}$*/Hrn* mice. This will allow the impaired hydroxylation machinery more time to convert chenodeoxycholic acid into β-muricholic acid. Indeed, Table 3 shows that the biliary bile salt composition in *Atp8b1*$^{G308V/G308V}$*/Hrn* mice is less hydrophobic than in *Abcb4*$^{-/-}$*/Hrn* mice because of a higher β-muricholate content and a lower chenodeoxycholate content. This secondary effect of cholestasis will further protect the cells against bile salt-induced damage. Thus, our data show that in PFIC cholestasis by secretory dysfunction is the primary mechanism whereas in the PFIC3 model, severe cellular damage to hepatocytes and cholangiocytes is caused by hydrophobic bile salts from the luminal side because biliary secretion is much less affected. It must be stressed that calculation of the hydrophobicity index of the plasma bile salts in single *Abcb4*$^{-/-}$ mice (Table 2) is prone to potentially large errors because these mice are not cholestatic and their plasma bile salt levels are exceedingly low.

Still, a comparison with the patient phenotypes is difficult. The bile salt pool of humans mainly consists of dihydroxy bile salts (chenodeoxycholate and deoxycholate) and $\sim$30% trihydroxy bile salts (cholate). This contrasts our CA-fed double transgenes, in which $>$90% of plasma and biliary bile salts are taurocholate and muricholate. We had expected a higher percentage of dihydroxy bile salts in the double transgenes. As mentioned above, a possible explanation for near absence of dihydroxy bile salts in the double transgenes may be that hepatic bile salt retention is enhanced because of cholestasis that, in combination with the 5% residual cytochrome *P*450 activity, renders rehydroxylation capacity sufficient to partially detoxify most dihydroxy bile salts (Table 2). Indeed, CA feeding of single transgenic *Hrn* mice resulted in a mole fraction dihydroxy bile salts of $\sim$20% (TCDC + TDC), whereas in the double transgenes CA supplementation of the diet resulted in a mole fraction dihydroxy bile salts of maximal 5% (Table 3). Another essential difference between mice and humans with regard to bile salt pool hydrophobicity is the nature of bile salt conjugation. In humans, $\sim$50% of bile salts are conjugated with glycine, whereas in mice bile salts are exclusively conjugated with taurine. Glycine-conjugated bile salts are more cytotoxic than taurine-conjugated bile salts, especially under mildly acidic conditions, that may occur in cholestasis.[27]

In conclusion, we have characterized new mouse models for PFIC1 and PFIC3 disease with a more hydrophobic bile salt pool composition. Mice developed pathology that better resembled the pathology observed in patients. We conclude that the bile salt pool composition is a critical determinant in the initiation and progression of cholestasis and liver pathology in PFIC1 and PFIC3.

Supplementary Information accompanies the paper on the Laboratory Investigation website (http://www.laboratoryinvestigation.org)

ACKNOWLEDGMENTS

We thank Dr Johanna Verheij for helpful discussions. This work was supported by a grant from the Dutch Digestive Disease Foundation (WO 08-63 to CCP).

DISCLOSURE/CONFLICT OF INTEREST

The authors declare no conflict of interest.

1. Morotti RA, Suchy FJ, Magid MS. Progressive familial intrahepatic cholestasis (PFIC) type 1, 2, and 3: a review of the liver pathology findings. Semin Liver Dis 2011;31:3–10.
2. Knisely AS. Progressive familial intrahepatic cholestasis: an update. Pediatr Dev Pathol 2004;7:309–314.
3. Pawlikowska L, Strautnieks S, Jankowska I, *et al.* Differences in presentation and progression between severe FIC1 and BSEP deficiencies. J Hepatol 2010;53:170–178.
4. Paulusma CC, Folmer DE, Ho-Mok KS, *et al.* ATP8B1 requires an accessory protein for endoplasmic reticulum exit and plasma membrane lipid flippase activity. Hepatology 2008;47:268–278.
5. Ujhazy P, Ortiz D, Misra S, *et al.* Familial intrahepatic cholestasis 1: studies of localization and function. Hepatology 2001;34(4 Pt 1):768–775.
6. Paulusma CC, Groen A, Kunne C, *et al.* Atp8b1 deficiency in mice reduces resistance of the canalicular membrane to hydrophobic bile salts and impairs bile salt transport. Hepatology 2006;44:195–204.
7. Trauner M, Fickert P, Wagner M. MDR3 (ABCB4) defects: a paradigm for the genetics of adult cholestatic syndromes. Semin Liver Dis 2007;27: 77–98.
8. Oude Elferink RP, Ottenhoff R, van Wijland M, *et al.* Uncoupling of biliary phospholipid and cholesterol secretion in mice with reduced expression of mdr2 P-glycoprotein. J Lipid Res 1996;37:1065–1075.
9. Oude Elferink RP, Paulusma CC, Groen AK. Hepatocanalicular transport defects: pathophysiologic mechanisms of rare diseases. Gastroenterology 2006;130:908–925.
10. Pawlikowska L, Groen A, Eppens EF, *et al.* A mouse genetic model for familial cholestasis caused by ATP8B1 mutations reveals perturbed bile salt homeostasis but no impairment in bile secretion. Hum Mol Genet 2004;13:881–892.
11. Smit JJ, Schinkel AH, Oude Elferink RP, *et al.* Homozygous disruption of the murine mdr2 P-glycoprotein gene leads to a complete absence of phospholipid from bile and to liver disease. Cell 1993;75: 451–462.
12. De Vree JM, Jacquemin E, Sturm E, *et al.* Mutations in the MDR3 gene cause progressive familial intrahepatic cholestasis. Proc Natl Acad Sci USA 1998;95:282–287.
13. Shah S, Sanford UR, Vargas JC, *et al.* Strain background modifies phenotypes in the ATP8B1-deficient mouse. PLoS One 2010;5:e8984.
14. Stapelbroek JM, Peters TA, van Beurden DH, *et al.* ATP8B1 is essential for maintaining normal hearing. Proc Natl Acad Sci USA 2009;106: 9709–9714.
15. Fickert P, Fuchsbichler A, Wagner M, *et al.* Regurgitation of bile acids from leaky bile ducts causes sclerosing cholangitis in Mdr2 (Abcb4) knockout mice. Gastroenterology 2004;127:261–274.
16. Benedetti A, Alvaro D, Bassotti C, *et al.* Cytotoxicity of bile salts against biliary epithelium: a study in isolated bile ductule fragments and isolated perfused rat liver. Hepatology 1997;26:9–21.
17. Rolo AP, Palmeira CM, Wallace KB. Interactions of combined bile acids on hepatocyte viability: cytoprotection or synergism. Toxicol Lett 2002;126:197–203.
18. Russell DW. The enzymes, regulation, and genetics of bile acid synthesis. Annu Rev Biochem 2003;72:137–174.
19. Nebert DW, Russell DW. Clinical importance of the cytochromes P450. Lancet 2002;360:1155–1162.
20. Henderson CJ, Otto DM, Carrie D, *et al.* Inactivation of the hepatic cytochrome P450 system by conditional deletion of hepatic cytochrome P450 reductase. J Biol Chem 2003;278:13480–13486.
21. Otto DM, Henderson CJ, Carrie D, *et al.* Identification of novel roles of the cytochrome p450 system in early embryogenesis: effects on vasculogenesis and retinoic acid homeostasis. Mol Cell Biol 2003;23: 6103–6116.
22. Kunne C, Acco A, Hohenester S, *et al.* Defective bile salt biosynthesis and hydroxylation in mice with reduced cytochrome P450 activity. Hepatology 2013;57:1509–1517.
23. Srivastava NK, Pradhan S, Mittal B, *et al.* An improved, single step standardized method of lipid extraction from human skeletal muscle tissue. Anal Lett 2006;39:297–315.
24. van Westrhenen R, de Waart DR, Akman S, *et al.* Assessment of peritoneal fibrosis by conventional light microscopy and hydroxyproline measurements. Perit Dial Int 2004;24:290–292.
25. Oude Elferink RP, Ottenhoff R, van WM, *et al.* Regulation of biliary lipid secretion by mdr2 P-glycoprotein in the mouse. J Clin Invest 1995;95:31–38.
26. van Nieuwerk CM, Groen AK, Ottenhoff R, *et al.* The role of bile salt composition in liver pathology of mdr2 (−/−) mice: differences between males and females. J Hepatol 1997;26:138–145.
27. Hohenester S, Wenniger LM, Paulusma CC, *et al.* A biliary HCO3- umbrella constitutes a protective mechanism against bile acid-induced injury in human cholangiocytes. Hepatology 2012;55:173–183.
28. Heuman DM. Quantitative estimation of the hydrophilic-hydrophobic balance of mixed bile salt solutions. J Lipid Res 1989;30:719–730.